



Title	On the Plastic Deformation of Single Crystal of Ice
Author(s)	WAKAHAMA, Gorow
Citation	Physics of Snow and Ice : proceedings, 1(1), 291-311
Issue Date	1967
Doc URL	<a href="http://hdl.handle.net/2115/20304">http://hdl.handle.net/2115/20304</a>
Type	bulletin (article)
Note	International Conference on Low Temperature Science. I. Conference on Physics of Snow and Ice, II. Conference on Cryobiology. (August, 14-19, 1966, Sapporo, Japan)
File Information	1_p291-311.pdf



[Instructions for use](#)

# On the Plastic Deformation of Single Crystal of Ice\*

Gorow WAKAHAMA

若 浜 五 郎

*The Institute of Low Temperature Science*

*Hokkaido University, Sapporo, Japan*

---

## Abstract

Experiments on the lateral extension and compression at constant strain rates were made with thin rectangular plates of single crystal of ice. The plates were 1 mm in thickness, 1~2 cm in width and 2~5 cm in length. Together with the observations through a polarizing microscope on the changes occurring in the ice crystal, the induced stress by extension or compression was electrically recorded.

Stress-strain curves thus obtained show that a single crystal of ice behaves in much the same manner as a perfect plastic body provided that it is strained at a rate below a certain critical value around 5% per hour. But this perfect plasticity can not be understood in the sense of the mathematical theory of plasticity, because the value of yield stress  $\sigma_Y$  depends upon the value of strain rate  $\dot{\epsilon}$  and  $\sigma_Y$  becomes smaller as  $\dot{\epsilon}$  diminishes.

Thus, the results of the experiments were interpreted by the theory of dislocation, taking into consideration the contraction of the force-measuring device, and that of the specimen. A linear relationship was found between  $v$ , the moving velocity of a dislocation line on the basal plane of ice crystal, and  $\tau$ , the shear stress acting upon it. The proportional constant  $v/\tau$  between the two was found to be  $3(\mu/\text{sec})/(\text{kg}/\text{cm}^2)$ .

The stress begins to relax at the moment when the extension or compression is terminated. If the time  $t$  is counted from that moment, between  $t$  and the relaxing stress  $\sigma$  the following relationship is found

$$1/\sigma = (1/\sigma_Y) + At. \quad (1)$$

The relaxation time  $\lambda$  depends upon  $\sigma_Y$  as well as upon  $\theta$  the angle between the crystallographic  $c$ -axis of the ice crystal and the direction of extension or compression. The larger  $\sigma_Y$  is, the shorter  $\lambda$  becomes. The theory of dislocation was applied successfully also to the phenomena of stress relaxation, giving exactly the above formula (1).

---

## I. Introduction

Plasticity of a single crystal of ice has extensively been studied by many workers since the end of the last century, and it was found that an ice crystal could easily change its shape by slipping along its basal planes (0001). But the slips occur quite unevenly in an ice crystal, that is to say, of the practically infinite number of basal planes only a few happen to become slip planes and the whole plastic deformation is apportioned to the large slips in them. In order to conduct a more detailed study on the plastic deformation of ice, experiments of extending and compressing thin plates of a single crystal of ice were carried out under a polarizing microscope with a force measuring device attached to the end of the plates. In this way the manner in which the slips develop

---

\* Contribution No. 803 from the Institute of Low Temperature Science.

could be observed in connection with the stress and strain brought about in the plates of ice crystal. The extension and compression were made at various constant speeds  $U$  within a temperature range from  $-3$  to  $-10^{\circ}\text{C}$ . As long as the time rate of change  $\dot{\epsilon}$  in strain was less than about 5% per hour, no distinction was found between the results of extension and compression except that the direction of slips and the sign of stress and strain were reversed. Hence, for the sake of brevity, the single word "compression" will be used in the sense of "compression and extension" or "compression or extension" in the preceding paragraphs.

Although the existence of dislocations in the basal planes of ice crystal has not yet been confirmed by direct experimental method, it is highly probable that the basal planes of ice crystal also slip on account of the movement of dislocation lines as in the case of other crystals. Results of the experiments on the thin ice plates were explained by the theory of dislocation. The explanation can be achieved by making use of only such results of the theory as learned from ordinary textbooks of dislocation.

## II. Experimental Methods

The experiments were carried out in a cold room by stretching and compressing thin rectangular plates of single crystal of ice in the direction of their longest sides. The plates were 1 mm in thickness, 1~2 cm in width and 2~5 cm in length. At first the single crystals from which the plates were to be cut out were grown artificially from water by means of Griggs-Coles' method, but afterwards natural single crystals brought from the Mendenhall glacier in Alaska to our laboratory were used. The cut was so made that the  $c$ -axis of the ice crystal always lay in the plane of the plates, with  $\theta$ , the

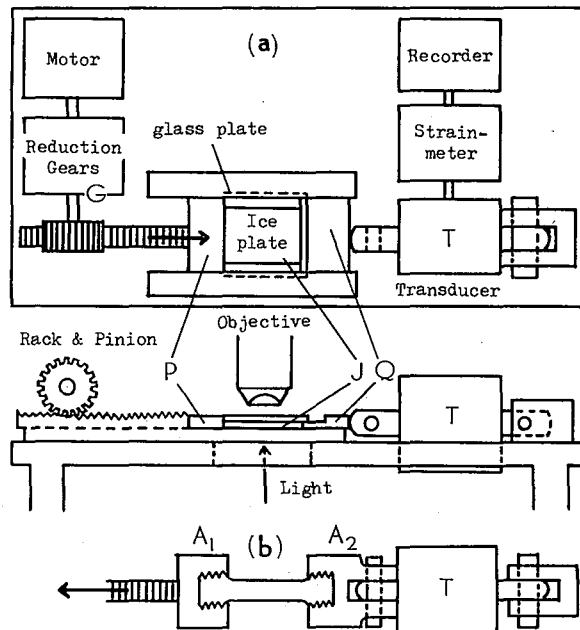


Fig. 1. Experimental apparatus for compressing and extending ice plates

angle between the  $c$ -axis and the direction of compression or extension was different from one plate to the other. After annealing at  $-5 \sim -10^\circ\text{C}$  for 24 hours, the ice plates were compressed or extended at slow constant strain rates of 1 to 10% per hour under a polarising microscope to observe the changes occurring in the ice crystals. Figure 1a shows schematically the apparatus used for the compression experiment. The ice plate J placed just below the objective lens of the microscope was pushed towards the right by a metal plate P which was driven by a synchronous motor M through a reduction gear system G. The stress brought about in the ice plate by the compression was transferred to the metal plate Q on the right. Transducer T of strain gauge type transformed the stress into electric current which was registered automatically on a sheet of recording paper. In the extension test, the ice plate was frozen to holders  $A_1$  and  $A_2$  at both ends and the holders were connected respectively to the head of a slowly moving rack and transducer T as shown in Fig. 1b. As the rack was moved slowly towards the left the ice plate was extended at constant speeds. The experiments were made in a cold room at temperatures  $-3$ ,  $-5$  and  $-10^\circ\text{C}$ .

### III. Results of the Experiment

#### 1) Stress-time curves

The thin plates of a single crystal of ice with  $\theta$  in the range  $20^\circ \sim 45^\circ$  give stress-time curves as schematically shown by curves OABC and OA'B'C' in Fig. 2. (The actual stress-time curves as they were recorded by the force measuring device are shown in the appendix at the end of this paper.) In the case of curve OABC the increasing rate  $\dot{\epsilon}'$  of strain is about 5% per hour, and in the case of curve OA'B'C'  $\dot{\epsilon}'$  is about 1% per

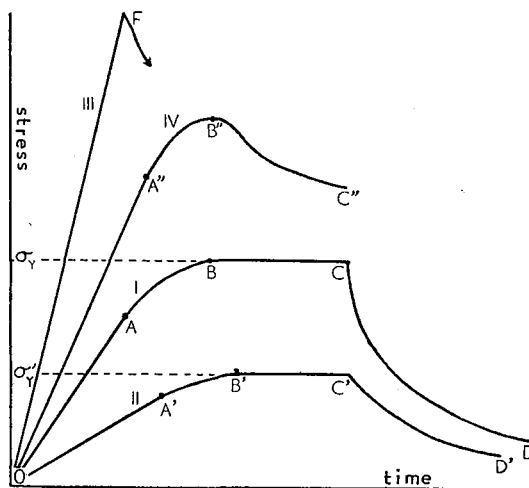


Fig. 2. Schematically drawn stress-time curves. I: Curve for  $\dot{\epsilon}' = 5\%$  per hour.  $\dot{\epsilon}'$  is the apparent time rate of change in strain, *i.e.*, the moving speed  $U$  of the left edge of the ice plate divided by its length  $L_0$ . Portions OA, AB, BC are called "first", "transient" and "steady" stages respectively. II: Curve for  $\dot{\epsilon}' = 1\%$  per hour. III: Curve for  $\dot{\epsilon} > 10\%$  per hour. The ice plate is broken at point F. IV: Curve with yield drop

hour. In both cases the stress  $\sigma$  in the ice plate linearly increases from point O up to points A or A', above which the increasing rate of the stress gradually decreases. The stage corresponding to OA or OA' of these stress-time curves will be called "the first stage of the experiments". After attaining  $\sigma_Y$  or  $\sigma'_Y$ , the so-called yield stress, at points B or B', the stress remains nearly constant even though the strain  $\epsilon'$  is still increasing. This stage will be called "the steady stage", because here  $\sigma$  is kept at the constant yield values  $\sigma_Y$  or  $\sigma'_Y$  steadily. The stage corresponding to the portions AB or A'B' of the stress-time curves will be named "the transient stage". Sometimes the yield drops; a drop in the stress immediately after the yield point, is observed in the last half of the transient stage as shown by curve OA''B''C''.

As time  $t$ , in the abscissa of the stress-time curves, is proportional to strain  $\epsilon'$ , the stress-time curves may be regarded as stress-strain curves of a single crystal of ice. The fact that the stress-strain curves have a "steady stage" suggests that a single crystal of ice behaves like a perfect plastic body, provided that it is strained at a rate less than 10% per hour. But this perfect plasticity could not be understood in the sense of the mathematical theory of plasticity, because the value of yield stress  $\sigma_Y$  depends upon the values of strain rate  $\dot{\epsilon}'$ . As seen from curves OABC and OA'B'C' in Fig. 2, the yield stress  $\sigma_Y$  becomes smaller as the strain rate  $\dot{\epsilon}'$  diminishes. Concerning the relationship between  $\sigma_Y$  and  $\dot{\epsilon}'$ , more detailed notes will be made in reference to Fig. 6 in section IV.

The strain and the time rate of its change denoted above by  $\epsilon'$  and  $\dot{\epsilon}'$  are  $\Delta x_0/L_0$  and  $U/L_0$ , where  $L_0$  is the length of the ice plates while  $\Delta x_0$  and  $U$  represent the displacement and the moving velocity of their left edge respectively. But  $\epsilon'$  and  $\dot{\epsilon}'$  thus defined are slightly different from the true strain and the true strain rate, for the right edge of the ice plates also moves if very slowly, as will be described in the next section. Therefore the above stated equivalence of the stress-time and stress-strain curves should be taken as an approximation. The stress  $\sigma$  is the ratio  $F/A_0$ , where  $F$  is the force measured through the force measuring device and  $A_0$  is the sectional area of the ice plates. As to  $\sigma$  there is no question.

## 2) Relaxation of stress

The stress  $\sigma$  begins to relax in such a fashion as shown by the portions CD and C'D' of the stress-time curves in Fig. 2, as soon as the compression (or extension) is stopped, that is to say, as soon as the movement of the left edge of the ice plate is stopped, at points C and C' in the steady stage of experiments. If the shear stress on the basal planes of the ice plates is denoted by  $\tau$ , it is connected with  $\sigma$  by the formula

$$\tau = \sigma \sin \theta \cos \theta. \quad (1)$$

In Fig. 3,  $1/\tau$  is plotted against time  $t$  counted from the moment at which the compression is stopped, for the three observed cases of relaxation. As seen from the figure, the experimental points are positioned along the straight lines. Therefore the relationship between  $\tau$  and  $t$  is given by

$$1/\tau = (1/\tau_Y) + A't, \quad (2)$$

where  $\tau_Y$  is the value of  $\tau$  in the steady stage of experiments and  $A'$  is a constant

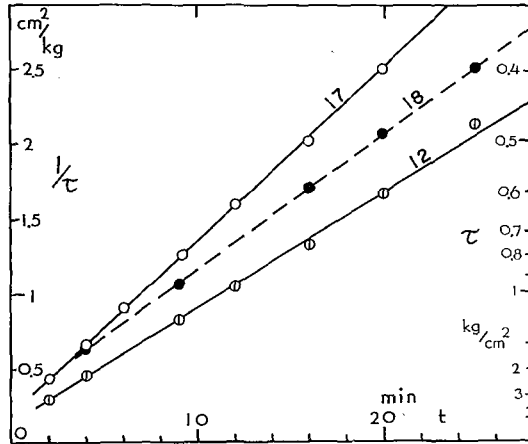


Fig. 3. Reciprocal of relaxing shear stress  $\tau$  on slip planes vs. time  $t$

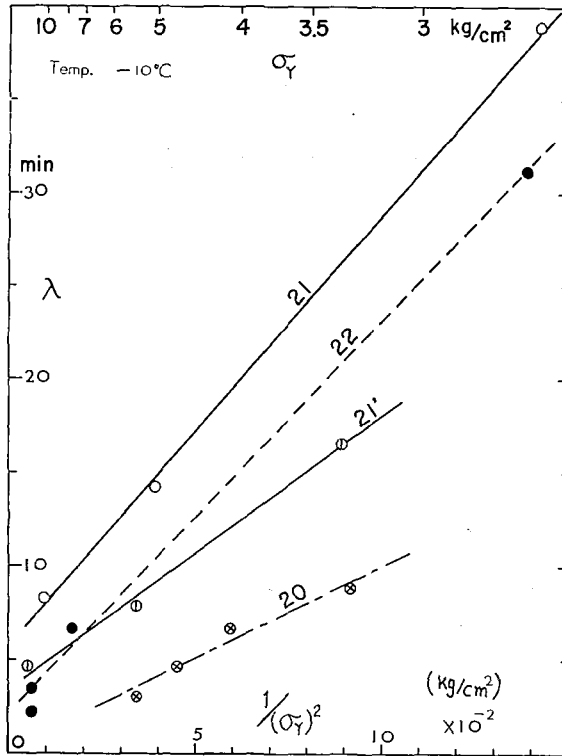


Fig. 4. Relaxation time  $\lambda$  vs. reciprocal of squared yield stress  $\sigma_Y^2$

dependent upon  $\tau_Y$  and temperature. If expressed in terms of  $\sigma$ , eq. (2) becomes

$$1/\sigma = (1/\sigma_Y) + At, \tag{3}$$

with  $A = A' \sin \theta \cos \theta$ .

The time interval during which  $\sigma$  is reduced to half  $\sigma_Y$  is given by

$$\lambda = 1/A \sigma_Y. \tag{4}$$

Let  $\lambda$  be called "relaxation time", although it departs somewhat from the general usage of the phrase. The longer  $\lambda$  is, the more slowly the stress relaxes.

For the same  $\theta$  and  $\sigma_Y$ ,  $\lambda$  becomes the longer, the more temperature is lowered. For  $\theta \sim 45^\circ$  and  $\sigma_Y = 5 \sim 10 \text{ kg/cm}^2$ ,  $\lambda$  which was  $2 \sim 3 \text{ min}$  at  $-4 \sim -5^\circ\text{C}$  rose to  $5 \sim 6 \text{ min}$  at  $-10^\circ\text{C}$ .

When  $\theta$  was near  $0^\circ$  or  $90^\circ$ ,  $\lambda$  was found to be very long. At  $-10^\circ\text{C}$ ,  $\lambda$  lay over a wide range extending from several hours to 30 hours.

At constant temperatures,  $\lambda$  changed in proportion to the reciprocal of  $\sigma_Y^2$ , namely,

$$\lambda \propto 1/\sigma_Y^2, \quad (5)$$

as shown in Fig. 4. The proportional constant depends upon  $\theta$  and the temperature.

### 3) Critical shear stress $\tau_c$

Relaxation of stress also occurs when the compression is interrupted at any point in the first stage of experiments except when the interruption is made too early after the beginning of the experiments. Curve EF in Fig. 5 shows the relaxation in such a case. As will be shown later in section VI, the relaxation of stress occurs on account of slips on the basal planes of ice crystal, that is to say, the relaxation is a manifestation of the plasticity of ice. Therefore, in the case of ice crystal, the linear relationship OA or OA' between stress and strain in the first stage of the stress-time curves in Fig. 2 does not represent pure elasticity. When a thin metal or glass plate was used in place of ice crystal, relaxation of stress was never observed so long as interruption of compression was made at such a point as corresponding to point E in Fig. 5.

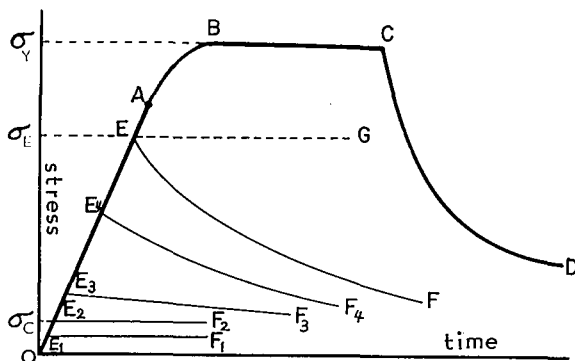


Fig. 5. Curves of stress relaxation starting from the first linear part of stress-time curve

The lower the point E lies at which the compression is interrupted on the line OA of Fig. 5, the more slowly the stress relaxes and finally relaxation becomes unobservable when point E comes to be positioned lower than a value  $\sigma_c$ . The value of  $\sigma_c$  depends on angle between the  $c$ -axis and the direction of compression. At  $-10^\circ\text{C}$ ,  $\sigma_c$  is given by  $\sigma_c = \tau_c / \sin \theta \cos \theta$ , if  $\tau_c$  is put equal to  $200 \text{ gr-wt/cm}^2$ . From this fact it may be said that the critical shear stress  $\tau_c$ , the smallest shear stress at which the basal planes of ice crystal begins to slip, lies around the value of  $200 \text{ gr-wt/cm}^2$  for temperatures not far apart from  $0^\circ\text{C}$ .

#### IV. Qualitative Explanation of Stress-Time Curves by the Theory of Dislocation

Kuroiwa and Hamilton showed by the use of chemical etching technique that some of the crystallographic planes of ice crystal other than the basal planes could slip. But such non-basal slips are very rare compared with the basal slips which occur quite easily. Therefore the above authors' finding does not affect the view that the plastic deformation of ice crystal is caused almost exclusively by the slips in its basal planes (0001). In terms of the theory of dislocation, this is the same as that where the dislocation lines in the non-basal planes can hardly move whereas those in the basal planes are almost free in moving. In the following sections the experimental results obtained above will be explained by assuming that the dislocation lines in the non-basal planes are entirely immovable.

##### 1) *Three dimensional network of dislocation lines*

It is assumed that the dislocation lines within an ice crystal make a three dimensional network. It is composed of segments of a dislocation line linked to one another at their ends. As the segments located in the non-basal planes do not move, those segments that lie in the basal planes have their ends firmly fixed and act as Frank-Read sources which generate new dislocation loops when subjected to a shear stress. The generated dislocation loops expand and give rise to successive slips on the basal planes to which the plastic deformation of the ice crystal is due.

##### 2) *Stress-time curve and stress-strain curve*

It was mentioned in article (1) of section III that the stress-time curves obtained by the experiments could be regarded as stress-strain curves, because the experiments were made by pulling or pushing the left edge of the ice plates at constant speeds  $U$ . But that change of expression was not right in the strict sense as noted at the end of the article. If the left edge of the ice plate was moved at constant speeds, the right edge was not completely fixed as it was connected to the force measuring device which was not rigid but was originally so constructed as to commence working when stretched or contracted. Let  $\Delta x_0$  and  $\Delta x_1$  be the respective displacements of the left and right edges of the ice plate. As the contraction  $\xi$  of the ice plate is equal to  $\Delta x_0 - \Delta x_1$ , that is,

$$\xi = \Delta x_0 - \Delta x_1, \quad (6)$$

the true strain  $\varepsilon$  of the ice plate is given by

$$\varepsilon = (\Delta x_0 - \Delta x_1) / L_0, \quad (7)$$

where  $L_0$  is the initial length of the ice plate. Consequently the true strain  $\varepsilon$  could be proportioned to  $\Delta x_0$  and the stress-time curves could become stress-strain curves, only when  $\Delta x_1$  were zero, in other words, only when the force measuring device were completely rigid.

Now, for the force measuring device to work, it must be stretched or contracted if it is to work at all, thus  $\Delta x_1$  can never vanish. But the stiffer the device, namely, the more sensitive a device is, the more  $\Delta x_1$  is reduced with the result that the stress-time curves approach the stress-strain curves.

3) *Active basal planes*

The figures a, b, c, ... of Fig. 6 illustrate the successive stages of slip development in the plate of ice crystal which is being compressed. The left edge of the plate moves rightwards at a constant speed  $U$  and, for the sake of convenience, the unit of time is so chosen that the edge shifts a distance equal to  $U$  from one stage to the next.

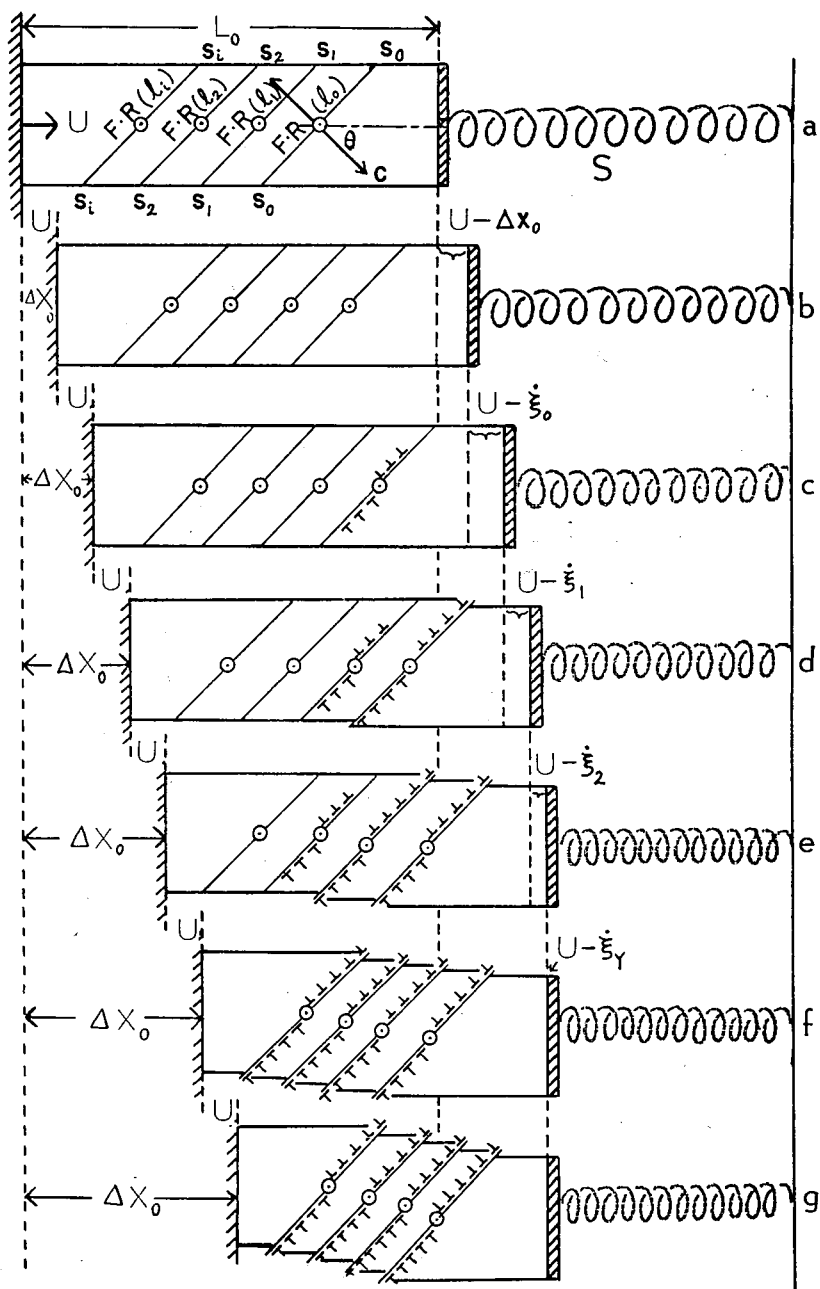


Fig. 6. Schema illustrating the development of slip planes in the ice plate

In other words, if  $j$  denotes an integer,  $\Delta x_0$  becomes equal to  $jU$  for each stage. Arrow C indicates the  $c$ -axis of the ice crystal which makes an angle  $\theta$  with the direction of compression. As the left edge of the ice plate moves, its right edge pushes the force measuring device represented by an imaginary spring S. The oblique straight lines marked  $s_0, s_1, s_2, \dots$  represent "active basal planes" in each of which a Frank-Read source is located as indicated by the dotted circle. A basal plane cannot always act as a slip plane even if it is provided with Frank-Read sources, because dislocations in the neighbouring basal planes may interfere with the motion of dislocations in the basal plane in question. And Frank-Read sources of very short length are practically inactive, for they require a very large shear stress to become active as will be seen in the next paragraph. But some of the basal planes will happen to be free from the interference and to have Frank-Read sources which are of sufficient length. Such basal planes can be slip planes and were mentioned previously as "active basal planes".

For a Frank-Read source to start generating new dislocation loops it needs be acted upon by a threshold shear stress of a magnitude of

$$\tau' = Gb/l, \quad (8)$$

where  $G$ ,  $b$  and  $l$  are respectively the rigidity of ice, the strength of Burgers vector and the length of the Frank-Read source. Let it be assumed that the Frank-Read sources in the active basal planes  $s_0, s_1, s_2, \dots$  are respectively of lengths of  $l_0, l_1, l_2, \dots$  and  $l_0 > l_1 > l_2, \dots$ . Then threshold stress  $\tau'_i = Gb/l_i$  needed for the Frank-Read source in the  $i$ -th active basal plane to begin working, increases as the number  $i$  becomes larger.

#### 4) *Successive participation in slipping of the active basal planes*

When the left edge of the ice plate in Fig. 6 begins to move at a constant speed  $U$ , every basal plane is sheared with the same shear stress  $\tau$  given by  $\sigma \sin \theta \cos \theta$ , where  $\sigma$  is the normal stress in the direction of the compression which is recorded through spring S. But, as long as  $\tau$  remains below  $\tau'_0 = Gb/l_0$ , none of the Frank-Read sources comes into play and the ice plate is compressed elastically. The second figure b of Fig. 6 shows the state in which the plate is contracted by  $\xi_0$  elastically. The third figure c shows the state where  $\tau$  has exceeded  $\tau'_0$  and the Frank-Read source in basal plane  $s_0$  has begun generating new dislocations to cause slips on that basal plane. If the rate  $\dot{\xi}_0$  at which the ice plate contracts due to those slips were large enough to cancel the advancing speed  $x_0$  of its left edge, its right edge would not move and the shear stress would be kept at the constant value  $\tau'_0$ . But  $\dot{\xi}_0$  is not so large as to compensate  $U$ , because the shear stress is small in the early stage of compression. Indeed the rate  $g$  of production of new dislocations by a Frank-Read source and their expanding velocity  $v$  are small for small values of shear stress. Therefore small shear stresses cannot cause large slips. Thus the right edge of the ice plate moves rightwards to contract the spring S and the shear stress  $\tau$  in the ice plate increases. Due to this increase in  $\tau$  the Frank-Read source on the next basal plane  $s_1$  starts working to cause that plane to slip. This state is shown in the fourth figure d of Fig. 6. In this way  $\tau$  keeps increasing to bring into successive play the Frank-Read sources in basal planes  $s_0, s_1, s_2, \dots$  and the contraction of the ice plate is more and more enhanced. Finally the contracting rate  $\dot{\xi}$  of the ice plate reaches  $U$  and the spring S stops contracting as

shown in figures f and g of Fig. 6.

Let  $m_Y$  basal planes be slipping in these final states. If the same number of dislocation loops as generated by the Frank-Read source are escaping off the ends of each slip plane, all the slip planes are filled with dislocation loops over the entire surface of their area as shown in figures f and g of Fig. 6. In such a situation, the ice plate contracts at a constant speed by the action of a constant stress, because each basal plane slips at a constant speed and no slip plane of the order higher than  $m_Y$  is needed for maintaining that constant contracting speed. In this way the ice plate comes finally to contract at the compressing speed  $U$  and the stress in it comes to be maintained at  $\sigma_Y$ .

##### 5) Correspondence between Figs. 2 and 6

The first portions near point O of the stress-time curves OABC and OA'B'C' in Fig. 2 correspond to the shift of state from figure a to figure b of Fig. 6, where the ice plate contracts elastically with no working Frank-Read sources. The critical shear stress  $\tau_c$  mentioned in article (3) of section III can be put equal to the threshold shear stress  $\tau'_0$  at which the first Frank-Read source on the basal plane  $s_0$  just begins to work.

The rise of stress following the above elastic portions in the stress-time curves of Fig. 2 corresponds to the successive participation in slipping of active basal planes  $s_0, s_1, s_2, \dots$  that occurs between stages b and f of Fig. 6. The final stages f and g of the compression give the horizontal parts of the stress-time curves, namely, the steady stage of the experiments, where normal stress  $\sigma$  is kept constantly at  $\sigma_Y$  or  $\sigma'_Y$ . If the contracting speed of the ice plate in this stage is denoted by  $\dot{\xi}_Y$ ,  $\dot{\xi}_Y$  is equal to  $U$ .

The curves OABC and OA'B'C' of Fig. 2 show that the steady stress  $\sigma_Y$  becomes larger as the ice plate is pushed at an increasing speed  $U$ . This fact can be explained as follows. Small  $U$  is compensated by a small contracting speed  $\dot{\xi}$  of the ice plate and the force measuring device stops contracting at a small degree of contraction. Therefore small  $U$  brings about a small  $\sigma_Y$ . By the same reason large  $U$  results in large  $\sigma_Y$ .

The value of steady normal stress  $\sigma_Y$  does not depend upon the stiffness of the force measuring device, because the device is not contracting in the steady stage of the compression. But the rise of stress in the first and transient stages of compression cannot be independent of the stiffness. By eq. (6) in article (2) of this section, contracting speed  $\dot{\xi}$  of the ice plate is, as  $d\Delta x_0/dt = \Delta \dot{x}_0 = U$ , given by

$$\dot{\xi} = \Delta \dot{x}_0 - \Delta \dot{x}_1 = U - \Delta \dot{x}_1, \quad (9)$$

where  $\Delta \dot{x}_1$ , the contracting speed of the force measuring device, becomes smaller with the increasing stiffness of the device. Therefore, for a given value of  $U$ ,  $\dot{\xi}$  is larger for a stiffer device and compensates  $U$  at an earlier time. Thus, the stiffer the device is, the more quickly the stress rises to attain the final value  $\sigma_Y$ , that is to say, the steeper the rise of stress in the first stage of experiments becomes.

## V. Moving Velocity of Dislocation Lines in the Basal Planes of Ice Crystal

There are many crystals in which the ends of dislocation lines appear as well-defined pits on their surfaces when etched by some suitable agents. In such crystals, the velocity

with which a dislocation line moves can be determined by microscopic observation of the displacement of its etch pit. In the case of an ice crystal, however, no one has ever succeeded in disclosing as etch pits the dislocations which lie in the basal planes, whereas those of the dislocations lying in non-basal planes have been discovered through etching by the authors referred to at the beginning of section IV. Therefore the method of etching cannot be used for obtaining the moving velocity of dislocations in the basal planes of ice crystal. But it is possible, as shown below, to determine its value through calculation by the aid of the theory of dislocation and by the use of number of the slip lines which were observed in the present experiments.

1) *Slipping velocity of a basal plane*

Let there be  $n'$  dislocation loops on a basal plane of which the length and the width are  $a$  and  $d$  respectively. If this is one of the basal planes of the thin ice plate used for the experiments,  $d$  is much shorter than  $a$ . Then each of the dislocation loops will take the form of a long rectangle of which the long sides coincide with the long sides of the basal plane, and the expansion of the loops will be executed by the advance of their ends both to the right and to the left. If the expanding or moving velocity of a dislocation loop, *i.e.* the velocity with which each of the elementary segments of the loop moves perpendicular to itself, is denoted by  $v$ , each loop in the basal plane extends its area by  $2dv$  in a unit time. Therefore the basal plane slips with the velocity

$$w' = b(2n'vd)/ad = 2n'bv/a, \quad (10)$$

where  $b$  is the Burgers vector of the dislocations lying in the basal planes of ice crystal.

As the normal line of the basal plane makes an angle  $\theta$  with the long sides of the ice plate as shown in Fig. 6,  $\dot{\xi}'$ , the speed of contraction of the ice plate caused by the above slip in the direction of compression, is expressed as

$$\dot{\xi}' = w' \sin \theta = 2n'bv \sin \theta/a.$$

If there are  $m$  slip planes and if the  $i$ -th slip plane has  $n'_i$  dislocation loops, the speed  $\dot{\xi}$  of contraction of the ice plate becomes

$$\dot{\xi} = (2bv \sin \theta/a) \sum_{i=0}^m n'_i. \quad (11)$$

Until now the slip planes have been distinguished by number  $i$ . After this, the threshold shear stress  $\tau'$  of Frank-Read source will be used for indicating the slip plane upon which that source is located, and the number of the Frank-Read sources in which the threshold stress lies between  $\tau'$  and  $\tau' + d\tau'$  will be expressed by

$$f(\tau') d\tau'. \quad (12)$$

Then eq. (11) is transformed into

$$\dot{\xi} = (2bv \sin \theta/a) \int_0^{\tau} n'(\tau') f(\tau') d\tau', \quad (13)$$

where  $n'(\tau')$  is the number of dislocation loops on the slip plane of the indication  $\tau'$ , and  $\tau$  is the threshold shear stress of the  $m$ -th Frank-Read source.

2) *Shear stress and contracting speed of the ice plate in the steady stage of experiments*

In the steady stage of compression of the ice plates where the stress-time curves

are horizontal straight lines, all of the slip planes are filled with dislocation loops as shown in figures f and g of Fig. 6. Let the shear stress and the speed of contraction of the ice plate in this stage be denoted by  $\tau_Y$  and  $\dot{\xi}_Y$  respectively. As noted in section IV,  $\dot{\xi}_Y$  is equal to  $U$ .

It is known that the mean spacing between the successive loops starting from a Frank-Read source of the length  $l$  is approximately equal to  $\pi l$ . Therefore, by eq. (8), the spacing  $\delta'$  of the loops generated by the Frank-Read source of the threshold shear stress  $\tau'$  becomes

$$\delta' = \pi b G / \tau' . \quad (14)$$

As the length of the slip planes is equal to  $a$ ,  $n'(\tau')$  is given by

$$n'(\tau') = a / \delta' = a \tau' / \pi G b , \quad (15)$$

and eq. (13) applied to the steady stage of experiments yields

$$U = \dot{\xi}_Y = (2v \sin \theta / \pi G) \int_0^{\tau_Y} \tau' f(\tau') d\tau' . \quad (16)$$

Let it be assumed that

$$f(\tau') = B , \quad (17)$$

where  $B$  is a constant independent of  $\tau'$ . Then the integration of eq. (16) gives

$$U = (B \sin \theta / \pi G) (v \tau_Y^2) . \quad (18)$$

### 3) Moving velocity of the dislocation lines in the basal plane of ice crystal

The number of slip planes in the ice plate could be determined by observation of slip lines through a microscope. The mean interval  $h_Y$  between the slip lines was found to be, in the steady stage of an experiment,

$$h_Y = 15 \mu \text{ for } \tau_Y = 3.2 \times 10^6 \text{ dyne} \cdot \text{cm}^{-2} . \quad (19)$$

The number of slip planes in the steady stage is equal to  $L_0 \cos \theta / h_Y$  on the one hand, and is given by  $B \tau_Y$  on the other. ( $L_0$  is the length of the ice plate.) Therefore, if  $\mu$  is used for representing  $B / L_0 \cos \theta$ ,

$$\mu = B / L_0 \cos \theta = 1 / \tau_Y h_Y , \quad (20)$$

and the numerical data eq. (19) give  $\mu$  the value

$$\mu = 2.2 \times 10^{-4} \text{ cm} \cdot \text{dyne}^{-1} . \quad (21)$$

The time rate of change in the longitudinal strain of the ice plate is given by  $\dot{\xi}_Y = U / L_0$  in the steady stage. The time rate of change  $\dot{\gamma}_Y$  in the shear strain of the slip planes is related to  $\dot{\xi}_Y$  by the relationship

$$\dot{\gamma}_Y = \dot{\xi}_Y / \sin \theta \cos \theta = (U / L_0) / \sin \theta \cos \theta , \quad (22)$$

and the elimination  $B$ ,  $U$  and  $L_0$  from eqs. (18), (20) and (22) yields

$$v = (\pi G / \mu) (\dot{\gamma}_Y / \tau_Y^3) \tau_Y . \quad (23)$$

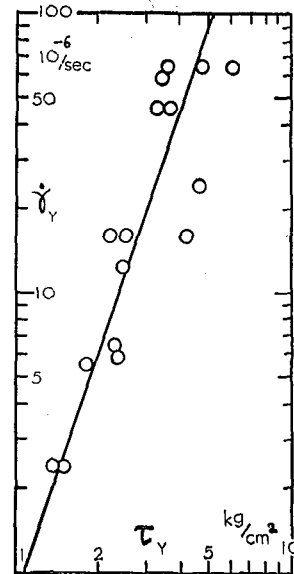


Fig. 7. Time rate of change  $\dot{\gamma}_Y$  in shear strain on slip planes in the steady stage of experiments vs. shear stress  $\tau_Y$  on slip planes in the same stage

In Fig. 7, the experimental values of  $\dot{\gamma}_Y$  and  $\tau_Y$  are plotted in logarithmic scales. Although the experimental points are scattered, they are positioned not very far from the straight line drawn in the figure, and this straight line gives

$$\dot{\gamma}_Y = \beta \tau_Y^3, \quad (24)$$

with

$$\beta = 7.3 \times 10^{-25} \text{ dyne}^{-3} \cdot \text{cm}^7 \cdot \text{sec}^{-1}. \quad (25)$$

Thus the final expression for the moving velocity  $v$  of the dislocation lines in the basal plane of ice crystal is obtained, from eqs. (23) and (24), as

$$v = k \tau, \quad (26)$$

with

$$k = \pi G \beta / \mu. \quad (27)$$

If  $G$ , the rigidity of ice, is put equal to  $3 \times 10^{10}$  dyne/cm<sup>2</sup> and the numerical values of  $\beta$  and  $\mu$  given above are used,  $k$  becomes

$$k = 3.1 \times 10^{-10} \text{ cm}^3 \cdot \text{sec}^{-1} \cdot \text{dyne}^{-1}. \quad (28)$$

Although the formula (26) was derived by use of the steady stage of experiments, it was only for the sake of convenience and the same formula should hold for any stage of compression or extension. For this reason  $\tau$  in eq. (26) is not suffixed with  $Y$  which indicates the steady stage.

The constant  $k$  will depend upon temperature. The value for  $k$  given above is valid for  $-10^\circ\text{C}$ , because the numerical data used in this section were only those of the

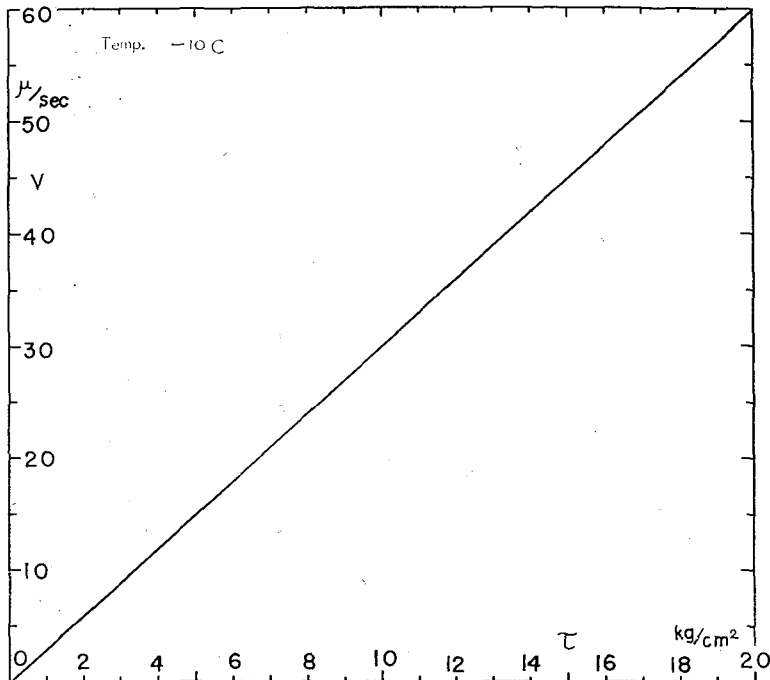


Fig. 8. Moving velocity  $v$  of dislocation lines vs. shear stress  $\tau$  on slip planes

experiments conducted at that temperature. The moving velocity  $v$  of dislocation lines expressed in the units of  $\mu/\text{sec}$  is plotted against the shear stress expressed in the units of  $\text{kg}/\text{cm}^2$  in Fig. 8. If  $\tau$  exceeds  $20 \text{ kg}/\text{cm}^2$ , the basal planes of ice crystal do not slip but break.

## VI. Relaxation of Stress

As mentioned in article (2) of section III, the stress  $\sigma$  in the ice plate begins to relax when the compression is stopped in the steady stage of experiments. If the movement of the left edge of the ice plate is stopped, the ice plate is still subject to the yield stress  $\sigma_Y$ . Due to this stress, slips are still occurring on the slip planes and the ice plate contracts. As the left edge of the ice plate is fixed, the contraction causes the force measuring device to extend with the result that the stress  $\sigma$  in the ice plate is diminished. By the same reasoning it will be understood that as long as there is a stress larger than the critical stress in the ice plate, it keeps contracting and the stress continues relaxing. If the relaxation of stress occurs in this way at all, its mode must be influenced by the stiffness  $\alpha$  of the force measuring device.

The strain  $\sigma$  in the ice plate is proportioned to the displacement  $\Delta x_1$  of its right edge, that is,

$$\sigma = \alpha \cdot \Delta x_1, \quad (29)$$

because  $\Delta x_1$  gives the contraction of the force measuring device. The stiffer the device is, the larger the constant  $\alpha$  is. In terms of  $\tau$ , this equation is written as

$$\tau = \alpha' \cdot \Delta x_1, \quad (30)$$

with  $\alpha' = \alpha \sin \theta \cos \theta$ . As the left edge of the ice plate is fixed in the case of stress relaxation, the contracting speed  $\dot{\xi}$  of the ice plate is equal to  $-d\Delta x_1/dt$ . Therefore the differential equation

$$\dot{\tau}/\alpha' = \dot{\xi}, \quad (31)$$

holds between  $\tau$  and  $\dot{\xi}$ . If  $\dot{\xi}$  is found as a function of  $\tau$  and time  $t$ ,  $\tau$  can be expressed as a function of  $t$  by the integration of this differential equation.

### 1) Formula for the relaxation of stress

As mentioned in article (2) of section III, it was found experimentally that the stress  $\sigma$  relaxes according to the formula

$$1/\sigma = (1/\sigma_Y) + At. \quad (32)$$

In order to approach this formula by the theory of dislocation, let the following two extreme cases (a) and (b) be considered.

(a) The case of an extremely small moving velocity of dislocation. Let the total number of the dislocation loops existing in the ice plate be denoted by  $n$ . Then, by eq. (13), the contracting speed  $\dot{\xi}$  is given by

$$\dot{\xi} = (2vb \sin \theta/a) n, \quad (33)$$

because  $\int_0^\tau n'(\tau')f(\tau')d\tau'$  in eq. (13) is nothing but the above total number. If the moving velocity  $v$  of the dislocation loops is extremely small, the dislocation loops disappearing

from the ice plate by escaping off the ends of the slip planes will be very few. Therefore  $n$  will remain almost equal to  $n_Y$ , the value of  $n$  at the beginning of relaxation, and the contracting speed of the ice plate can be written as

$$\dot{\xi}_a = (kB \sin \theta / \pi G) \tau_Y^2 \tau, \quad (34)$$

because  $v = k\tau$  (eq. (26)),  $f(\tau') = B$  (eq. (17)),  $n'(\tau') = a\tau' / \pi bG$  (eq. (15)) and  $n_Y$  is given by

$$n_Y = \int_0^{\tau_Y} n'(\tau') f(\tau') d\tau' = (aB/2\pi bG) \tau_Y^2. \quad (35)$$

(b) The case of an extremely large moving velocity of dislocation. When the dislocation loops move extremely fast, slip planes become empty of dislocation loops unless the Frank-Read sources located on them are generating dislocations. On the other hand, if the Frank-Read source is generating dislocation loops, the slip plane on which the source is located is filled with the loops. A Frank-Read source can generate dislocation loops when its threshold stress  $\tau'$  is smaller than  $\tau$ . Therefore, in the case of an extremely large  $v$ , the total number  $n$  of the dislocation loops existing in the ice plate is given by

$$n = \int_0^{\tau} n'(\tau') f(\tau') d\tau' = (aB/2\pi bG) \tau^2, \quad (36)$$

and the contracting speed of the ice plate becomes

$$\dot{\xi}_b = (kB \sin \theta / \pi G) \tau^3. \quad (37)$$

Since actual cases must be intermediate between the above two extreme cases, let it be assumed that the actual contracting speed  $\dot{\xi}$  of the ice plate is given by the geometrical mean of  $\dot{\xi}_a$  and  $\dot{\xi}_b$ :

$$\dot{\xi} = \sqrt{\dot{\xi}_a \dot{\xi}_b} = (kB \sin \theta / \pi G) \tau_Y \tau^2. \quad (38)$$

Then the combination of eqs. (31) and (38) yields

$$\dot{t} = -A' \tau^2, \quad (39)$$

with

$$A' = \alpha kB \sin \theta \tau_Y / \pi G, \quad (40)$$

from which is obtained by integration the equation

$$1/\tau = (1/\tau_Y) + A't. \quad (41)$$

Here  $t$  is the time counted from the moment when the compression of the ice plate is stopped and  $\tau_Y$  is the yield shear stress in the steady stage of experiments. If  $\tau$  is transformed into  $\sigma$ , eq. (41) becomes eq. (3) which was found by the experiments to be the formula connecting the relaxing stress  $\sigma$  with time  $t$ .

## 2) The relaxation time $\lambda$ and the yield shear stress $\tau_Y$

In article (2) of section III, the relaxation time was defined as  $\lambda = 1/\sigma_Y A$ , which is transformed into

$$\lambda = 1/\tau_Y A', \quad (42)$$

if  $\tau_Y$  is used in place of  $\sigma_Y$ . The above obtained expression (40) for  $A'$  turns eq. (42) into

$$\lambda = C/\tau_Y^2, \quad (43)$$

with

$$C = \pi G / \alpha k B \sin \theta. \quad (44)$$

It was shown in article (2) of section III that the values of  $\lambda$  and  $\tau_Y$  found by the experiments were related to each other in the form of eq. (43). As  $\lambda$  is inversely proportioned to  $\alpha$ , the stiffer the force measuring device is, the faster the stress relaxes.

### VII. Linear Rise of Stress-Time Curves in the First Stage of Experiments

In this section an explanation will be given to the fact that the stress  $\sigma$  in the ice plates rises in proportion to time  $t$  in the first stage of the experiments.

#### 1) Fashion of change in the contracting speed $\dot{\xi}$ of the ice plate

As  $\sigma$  increases in proportion to  $\tau$  as well as to  $\Delta x_1$  in eq. (6) of section IV, that equation can be rewritten as

$$\tau / \alpha' = \Delta x_0 - \xi, \quad (45)$$

where  $\alpha'$  is the same constant as introduced in the previous section. Through differentiation with respect to time  $t$ , eq. (45) becomes

$$\dot{\tau} / \alpha' = U - \dot{\xi}, \quad (46)$$

where  $U$  stands for  $\Delta \dot{x}_0$ , the constant speed at which the left edge of the ice plate moves. If  $\dot{\tau}$  is a constant,  $\dot{\sigma}$  is a constant and  $\sigma$  increases in proportion to  $t$  as stated above at the beginning of this section. It will be seen from eq. (46) that there can be two possible cases for  $\dot{\tau}$  to be a constant: first, that  $\dot{\xi}$  is a constant comparable with  $U$  in magnitude, and secondly, that  $\dot{\xi}$  changes within a limit lying far below  $U$ , i.e.  $\dot{\xi}$  is subject to the condition  $\dot{\xi} \ll U$ . In the second case  $\dot{\tau}$  is not strictly a constant but can practically be regarded as such, and this very case was found to be true by the following experiments.

A plate of glass is very hard compared with an ice plate and contracts just a little if compressed, namely,  $\dot{\xi}$  is very small for a glass plate. Experiments of compression were made by the use of a glass plate in place of the ice plates. The stress-time curves obtained were straight lines and their inclination was found to be the same as that of the first straight portion of the stress-time curves of ice plates for any value of the compressing speed  $U$ . This fact shows that the condition  $\dot{\xi} \ll U$  is satisfied in the first stage of the experiments on the ice plates. Thus it was learned in the case of ice plates that  $\dot{\xi}$  remains small for a while after the beginning of experiments and then begins to increase rapidly until it becomes great enough to cancel the advancing speed  $U$  of the left edge of the ice plates. Such a fashion of change in  $\dot{\xi}$  can be explained by the theory of dislocation as will be described below.

#### 2) Number of dislocation loops generated by the Frank-Read sources

As assumed in article (2) of section V, let the number of Frank-Read sources of which the threshold stress lies between  $\tau'$  and  $\tau' + d\tau'$  be

$$f(\tau') d\tau' = B d\tau'. \quad (47)$$

Let the number of dislocation loops, which are generated per unit time by a shear stress  $\tau$  from a Frank-Read source of the threshold stress  $\tau'$ , be denoted by  $g(\tau, \tau')$ . Then, by eqs. (14) and (26),  $g(\tau, \tau')$  is known to be

$$g(\tau, \tau') = \frac{v}{\delta'} = \frac{k}{\pi Gb} \tau \tau', \quad (48)$$

and the number  $dn$  of those dislocation loops, that have started up till the time  $t$  from the Frank-Read sources of the threshold stress lying between  $\tau'$  and  $\tau' + d\tau'$  and are existing at that time, is given by

$$\begin{aligned} dn &= B d\tau' \int_{t'}^t g(\tau, \tau') dt \\ &= \frac{kB}{\pi Gb} \tau' d\tau' \int_{t'}^t \tau dt, \end{aligned} \quad (49)$$

where  $t'$  is the time at which the shear stress reached  $\tau'$ . If it is assumed that

$$\tau = pt, \quad (50)$$

namely, that the shear stress increases in proportion to time  $t$ , eq. (49) is transformed into

$$dn = (kB/2\pi b pG) \tau' (\tau^2 - \tau'^2) d\tau', \quad (51)$$

with  $\tau' = pt'$ . Then  $n$ , the total number of the dislocation loops existing in the ice plate at time  $t$ , is given by

$$n = \int dn = \frac{kB}{2\pi Gbp} \int_0^\tau \tau' (\tau^2 - \tau'^2) d\tau' = (kB/8\pi b pG) \tau^4. \quad (52)$$

### 3) The proportional limit

The use of the above value for  $n$  in eq. (33) in section VI yields the contracting speed  $\dot{\xi}$  of the ice plate as

$$\dot{\xi} = \frac{vkB \sin \theta}{4\pi Gap} \tau^4 = \frac{k^2 B \sin \theta}{4\pi Gap} \tau^5, \quad (53)$$

and from this the following relationship is obtained between  $\dot{\xi}/U$  and time  $t$ :

$$\frac{\dot{\xi}}{U} = (Kt)^5, \quad K = \left[ \frac{k^2 B \sin \theta p^4}{4\pi GUa} \right]^{1/5}. \quad (54)$$

It is seen from this relationship that  $\dot{\xi}/U$  is very small for small values of  $t$  and begins to increase rapidly when  $Kt$  approaches 1. For  $Kt < 0.65$ ,  $\dot{\xi}/U$  is less than 0.1. Therefore it may be said that the condition  $\dot{\xi} \ll U$  is satisfied and  $\tau$  increases in proportion to  $t$  until  $t$  attains the value  $t_l = 0.65/K$ . In this way the stress-time curves start in the form of straight lines as actually shown by the experiments. Let the value of  $\tau$  at  $t_l$  be denoted by  $\tau_l$ . The suffix  $l$  is used for indicating the values at the "proportional limit", the upper limit of the first stage of stress-time curves marked A and A' in Fig. 2.

The value of  $\dot{\tau}$  is found to be equal to  $p$  from eq. (50) on the one hand and equal to  $\alpha'U$  from eq. (46) on the other by disregarding  $\dot{\xi}$  against  $U$ . Thus

$$p = \alpha' U, \quad (55)$$

and this relation transforms  $K$  into

$$K = \left[ \frac{k^2 B \alpha'^4 U^3 \sin \theta}{4\pi Ga} \right]^{1/5}, \quad (56)$$

which gives

$$K \propto U^{3/5}. \quad (57)$$

Since  $t_l = 0.65/K$ , it is seen from this relation that the earlier the linear rise of stress

finishes, the larger the compressing speed  $U$  is.

Equation (53) can be put in the form

$$\frac{\dot{\xi}}{U} = \frac{k^2 B \sin \theta}{4\pi G a \alpha'} \cdot \frac{\tau^5}{U^2}. \quad (58)$$

As  $\dot{\xi}/U=0.1$  and  $\tau=\tau_l$  at the proportional limit, the relation

$$\tau_l \propto U^{2/5}, \quad (59)$$

is drawn out from eq. (58). The shear stress at the proportional limit rises as the compressing speed  $U$  increases.

#### 4) Number of slip planes

The assumptions of  $f(\tau')=B$  and  $\tau=pt$  require that the same number of Frank-Read sources should start working in any of the unit times during the first stage of experiments. Let the interval between the starting times of any two successive Frank-Read sources be denoted by  $q$ . Then the number of the Frank-Read sources working at time  $t$  is given by  $t/q$  on the one hand and by  $B\tau$  on the other. Thus, by eqs. (50) and (55),  $q$  is obtained as

$$q = t/B\tau = 1/BU\alpha'. \quad (60)$$

The number of slip planes is the same as that of the Frank-Read sources which are working. At the proportional limit, there are

$$m_l = t_l/q = 0.65/qK, \quad (61)$$

slip planes. Equations (57) and (60) show that  $m_l$  is proportioned to  $U$ , that is,

$$m_l \propto U^{2/5}, \quad (62)$$

which relationship can also be derived from eq. (59) and the assumption  $f(\tau')=B$ .

Beyond the proportional limit, the assumption of  $\tau=pt$  becomes invalid. Another assumption such as  $\tau \propto t^M$  with  $M > 1$  will fit, and  $\dot{\xi}$  will come to increase much more rapidly than it does in accord with eq. (54).

#### 5) Numerical example

In this article, the quantities introduced or deduced above will be given numerical values in regard to one of the experiments actually made by the present author.

The quantities concerning the ice plate and the experimental device were:

$U=4 \times 10^{-5}$  cm·sec<sup>-1</sup>, compressing speed,

$\alpha=10^9$  dyne·sec·cm<sup>-3</sup>, stiffness of the force measuring device,

$a=2$  cm, length of each of the slip planes,

$\theta=45^\circ$ , angle between the  $c$ -axis of the ice plate and the direction of compression,

$k=3.1 \times 10^{-10}$  cm<sup>3</sup>·dyne<sup>-1</sup>·sec<sup>-1</sup>, proportional constant relating the moving velocity  $v$  of dislocation lines with shear stress  $\tau$ . This value of  $k$  was determined in section V.

By the experiment it was found that

$p=4 \times 10^4$  dyne·cm<sup>-2</sup>·sec<sup>-1</sup>, proportional constant between shear stress  $\tau$  and time  $t$ ,

$q=3.3 \times 10^{-2}$  sec, time interval between the starting times of two successive Frank-Read sources.

The time interval  $q$  was determined by counting through the microscope the new slip lines that became visible during a definite time.

The above numerical values put in eq. (56) give

$$K = 0.86 \times 10^{-2} \text{ sec}^{-1},$$

from which are obtained

$$t_i = 76 \text{ sec} \quad \text{and} \quad m_i = 2100.$$

These calculated values were in good accord with those determined experimentally.

### Acknowledgments

The author wishes to express his deep appreciation of the stimulating suggestions and discussions to Prof. Zyungo Yosida. Thanks are also due to the members of the research group for snow and ice in this Institute. Helpful discussions and criticisms were provided by Prof. Hideji Suzuki of the Tokyo University. This work was partially supported by the Grant-in-Aid for Fundamental Scientific Research from the Ministry of Education.

### References

- 1) COTTRELL, A. H. 1953 Dislocations and Plastic Flow in Crystals, University Press, Oxford, 223 pp.
- 2) KUROIWA, D. and HAMILTON, W. L. 1963 Studies of ice etching and dislocation etch pits. *In Ice and Snow* (W. D. KINGERY, ed.), M. I. T. Press, Cambridge, Mass., 34-55.
- 3) NAKAYA, U. 1958 Mechanical properties of single crystals of ice, I. *SIPRE Res. Rept.*, **28**, 1-44.
- 4) WAKAHAMA, G. 1962 On the plastic deformation of ice, I~IV. *Low Temp. Sci.*, **A 20**, 57-130.\*
- 5) YOSIDA, Z. and WAKAHAMA, G. 1962 Models of dislocations in ice crystal. *Low Temp. Sci.*, **A 20**, 29-56.\*

\* In Japanese with English summary.

## Appendix

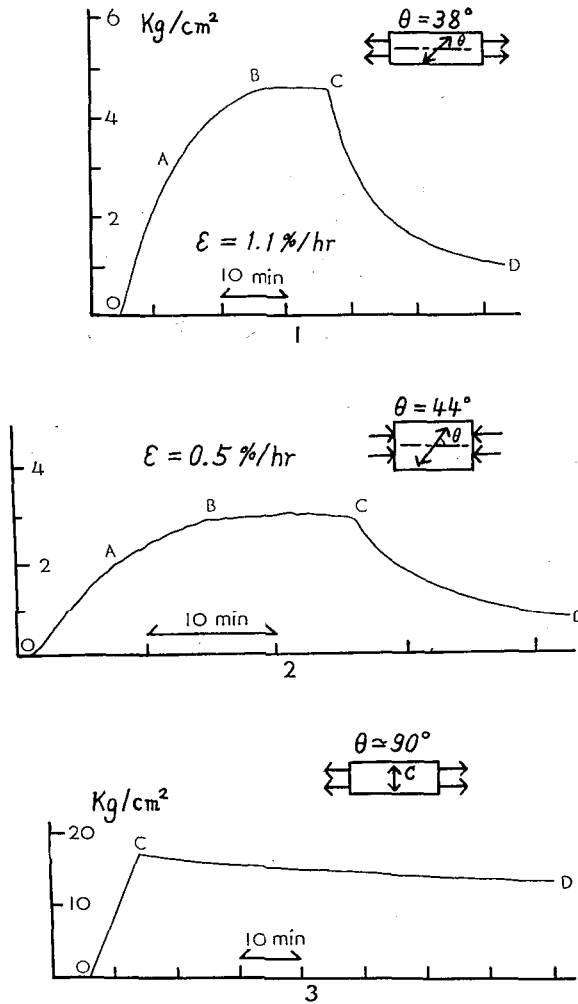
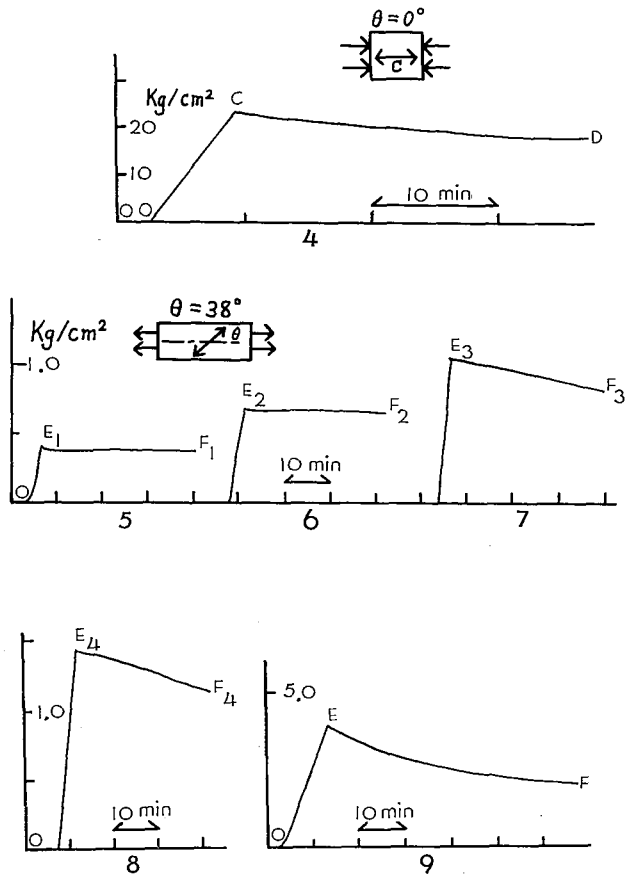


Fig. 9 a. Traces of the actual stress-time curves and stress relaxation curves of single crystals of ice

- 1, 2: Typical stress-time curve OABC and stress relaxation curve CD
- 3: Stress relaxation curve CD in special case



**Fig. 9 b.** Traces of the actual stress-time curves and stress relaxation curves of single crystals of ice

4: Stress relaxation curve CD in special case

5, 6, 7, 8, 9: Stress relaxation curves  $E_1F_1, \dots, E_4F_4, EF$ . These curves respectively correspond to the curves  $E_1F_1, \dots, EF$  in Fig. 5 of the text